Dissecting the roles of GRK2 and GRK3 in μ-opioid receptor internalization and β-arrestin2 recruitment using CRISPR/Cas9-edited HEK293 cells

Authors:

Mie F. Pedersen[1,3], Thor C. Møller[1,3*], Sofie D. Seiersen[1], Jesper M. Mathiesen[1], Michel Bouvier[2], Hans Bräuner-Osborne[1*].

[1]*Department of Drug Design and Pharmacology, University of Copenhagen, 2100 Copenhagen, Denmark.*

[2]*Department of Biochemistry and Molecular Medicine, Institute for Research in Immunology and Cancer, Université of Montréal, Montreal, QC, Canada*

[3]These authors contributed equally to this work

*Co-corresponding authors: thor.moller@sund.ku.dk; hbo@sund.ku.dk

Abstract

Most G protein-coupled receptors (GPCRs) recruit β-arrestins and are internalized upon agonist stimulation. For the μ-opioid receptor (μ-OR), this process has been linked to development of opioid tolerance. GPCR kinases (GRKs), particularly GRK2 and GRK3, have been shown to be important for μ-OR recruitment of β-arrestin and internalization. However, the contribution of GRK2 and GRK3 to β-arrestin recruitment and receptor internalization, remain to be determined in their complete absence. By CRISPR/Cas9 we established HEK293 cells with knock-out of GRK2, GRK3 or both to dissect their individual contributions in β-arrestin2 recruitment and μ-OR internalization upon stimulation with four different agonists. We showed that GRK2/3 removal reduced agonist-induced μ-OR internalization substantially. Furthermore, we found GRK2 to be more important for μ-OR internalization than GRK3. In contrast, the effect of GRK2/3 knock-out on β-arrestin2 recruitment was minor. Rescue expression experiments restored GRK2/3 functions. The GRK2/3 small molecule inhibitor CMPD101 showed a high similarity between the genetic and pharmacological approaches, cross-validating the specificity of both. However, off-target effects were observed at high CMPD101 concentrations. These GRK2/3 KO cell lines should prove useful for a wide range of studies on GPCR function.

Introduction:

The family of G protein-coupled receptors (GPCRs) constitute important drug targets, through which ~30% of all clinically approved medicines mediate their action[1]. Regulation of GPCR signaling following receptor activation is a complex process that typically involves recruitment of kinases that phosphorylate the receptor, which increases the affinity for β-arrestins and mediate receptor internalization[2]. The μ-opioid receptor (μ-OR) belongs to the family of rhodopsin-like (family A)

GPCRs and mediates the analgesic effects of opioid drugs and related side-effects and addictive properties[3,4]. The regulation of μ-OR desensitization and trafficking has been suggested to be linked to the development of tolerance after chronic use of opioid drugs[5] and it is therefore important to understand the underlying molecular mechanisms.

Several studies indicate that receptor phosphorylation by GPCR kinases (GRKs) is important for the desensitization of μ-OR signaling and initiation of internalization[6–9]. Out of the seven isotypes in the GRK family, four (GRK2, GRK3, GRK5 and GRK6) have been speculated to regulate μ-OR *in vivo* due to their overlapping expression patterns[10]. Knock-out (KO) models have confirmed the importance of the individual GRKs. For instance, it has been demonstrated that fentanyl and morphine-induced tolerance are decreased in GRK3 KO mice[11], morphine reward and dependence are lost in mice depleted of GRK5, but not GRK3, and morphine-induced locomotor activity is increased in mice lacking GRK6 compared to wild type littermates[12,13]. Altogether, these studies suggest that phosphorylation of μ-OR by specific GRK subtypes differentially impacts the physiological outcome upon stimulation with opioids. The role of GRK2 has not been addressed in KO systems due to lethal effects of removing GRK2 in mouse embryos[14]. Instead, the role of GRK2 has been studied using e.g. perfusion of a GRK2-inhibitory peptide or overexpression of a GRK2 dominant negative mutant in rat neurons, both demonstrating a role of GRK2 in μ-OR desensitization[15,16].

Further insights into the mechanisms behind the role of GRKs in μ-OR pharmacology has been obtained from *in vitro* studies. An early study demonstrated that phosphorylation of the μ-OR could be increased by GRK2 overexpression, which led to increased β-arrestin recruitment and μ-OR internalization[17]. The involvement of μ-OR phosphorylation in these processes was confirmed by later studies[18–21]. In addition to GRK2, *in vitro* studies have shown that GRK3/5/6 have direct roles

in μ-OR phosphorylation and/or internalization[13,20,22–24]. Moreover, studies have also utilized phospho-site specific antibodies to demonstrate that the μ-OR is differentially phosphorylated by distinct GRK isotypes depending on the agonist used. For instance, stimulation with the agonist D-Ala(2)-mephe(4)-gly-ol(5))enkephalin (DAMGO) leads to phosphorylation of T370, S375, T376 and T379 in mouse μ-OR whereas stimulation with morphine only leads to phosphorylation of S375[20,23]. In the same studies, the relative contribution of GRK2/3/5/6 to μ-OR phosphorylation was also dependent of the agonist used.

The tools to study the involvement of GRKs in cell systems, has for now been restricted mainly to short-interfering RNA techniques[20,23], the usage of dominant negative mutants of GRK2[17,25] and utilization of Takeda compound 101 (CMPD101), a reported GRK2/3 selective inhibitor[26–28]. To the best of our knowledge, no studies have investigated the role of GRKs in μ-OR internalization in cell systems with complete KO of specific GRKs, which would prevent incomplete knockdown of expression, residual kinase activity or unwanted overexpression effects.

Here, we report construction of individual and double KO of GRK2 and GRK3 cell lines in the human embryonic kidney 293A (HEK293A) background, which we employ to investigate the agonist-induced μ-OR internalization and β-arrestin2 recruitment in response to four different agonists. We find that KO of GRK2 and GRK3 reduces agonist-induced μ-OR internalization without affecting β-arrestin2 recruitment to the membrane of HEK293A cells. Furthermore, we present a side-by-side comparison of the effects obtained with CMPD101 to the responses obtained in GRK2/3 double KO cells. We find highly similar results with the two approaches when 10 μM of CMPD101 is used; higher CMPD101 concentrations lead to non-GRK2/3-mediated effects. The cell lines provide full KO of two important regulators of GPCR function and we expect them to be useful tools for future studies of GPCR function.

Results

Validation of GRK2 and/or GRK3 genome-edited HEK293A cells

Construction of individual and combined GRK2 and GRK3 KO HEK293A cells (ΔGRK2, ΔGRK3 and ΔGRK2/3) were performed using the clustered regularly interspaced short palindromic repeats (CRISPR)/CRISPR associated protein 9 (Cas9) technology. Clones containing complete modification of all alleles were identified with insertions or deletions in the *ADRBK1* locus (GRK2) and/or the *ADRBK2* locus (GRK3) leading to frameshifts as shown by sequencing and indel detection by amplicon analysis (IDAA). Furthermore, we confirmed the absence of full-length GRK2 protein expression in the ΔGRK2 and ΔGRK2/3 cells and of full-length GRK3 protein expression in the ΔGRK3 and ΔGRK2/3 cells using GRK2- and GRK3-selective antibodies (**Fig. 1**). No alteration of GRK2 expression in the ΔGRK3 clone or GRK3 expression in the ΔGRK2 clone compared to parental cells could be detected (**Fig. 1**).

GRK2 and GRK3 contributes to μ-OR internalization

We used a real-time internalization assay to determine the influence of GRK2 and GRK3 on μ-OR internalization. This assay is based on time-resolved Förster resonance energy transfer (TR-FRET) between a long lifetime donor (Lumi4-Tb) covalently linked to an amino-terminal SNAP-tag on cell surface μ-OR and a cell impermeant acceptor (fluorescein) in the extracellular buffer[29,30]. Internalization separates the donor and acceptor molecules thus preventing energy transfer and increasing the ratio of donor over acceptor emissions (internalization ratio). We compared the ability of four μ-OR agonists to stimulate internalization: DAMGO, loperamide, fentanyl and morphine. All four agonists induced internalization in a concentration-dependent manner and

reached a plateau between 45 and 90 min after agonist addition in the parental HEK293A cells as well as in the ΔGRK2, ΔGRK3 and ΔGRK2/3 cell lines (**Fig. 2, Supplementary Fig. S1**). Internalization was clearly reduced in the ΔGRK cells with DAMGO, loperamide and fentanyl stimulation. A similar tendency was observed for morphine, but the effect was less clear compared to the three other agonists due to lower overall internalization levels with morphine stimulation. A cell line where β-arrestin1 and -2 have been deleted in the same cellular background as the ΔGRK cell lines has previously been described[31]. None of the agonists were able to induce internalization in the Δβ-arrestin1/2 cell line (**Fig. 2, Supplementary Fig. S1**). We used the area under the curve from the 90 min real-time internalization ratio traces to plot concentration-response curves and determine the maximum response (E_{max}) and potency (EC_{50}) for the four agonists in each of the cell lines where internalization could be detected (**Fig. 2, Table 1**). For DAMGO, fentanyl and loperamide, we found a decrease in E_{max} compared to the parental cells of 48-62% and 22-23% in the ΔGRK2 and the ΔGRK3 cell lines, respectively. The E_{max} was further reduced, but not completely abolished in the ΔGRK2/3 cell line and corresponded approximately to the sum of the reductions in the individual ΔGRK2 and ΔGRK3 cell lines. The responses to morphine stimulation were too small for quantitative analysis. Importantly, there were no differences between the μ-OR surface expression in the parental cells and the ΔGRK2 and/or -3 cell lines (**Fig. 2e**). To determine whether the reduced internalization was due to off-target effects of the single guide RNAs (sgRNAs) we overexpressed the deleted GRKs in the corresponding cell lines. GRK2 or -3 overexpression restored the internalization ratio to the levels of the parental cells or higher, thus showing that the internalization machinery is fully functional in the ΔGRK cell lines (**Supplementary Fig. S2**).

GRK2 and GRK3 deletion does not reduce β-arrestin2 recruitment

To further investigate the mechanism linking GRK2/3 and μ-OR internalization we measured the recruitment of β-arrestin2 to μ-OR in the ΔGRK2 and/or -3 cells using an enhanced bystander bioluminescence resonance energy transfer (ebBRET) assay[32]. In this assay, BRET between *Renilla reniformis* luciferase II (RlucII)-tagged β-arrestin2 and a membrane anchored *R. reniformis* GFP (rGFP) increases when β-arrestin2 is recruited to the membrane. Importantly, no modification of the intracellular domains of the receptor is required for this assay. We compared the ability of DAMGO, fentanyl, loperamide and morphine to induce β-arrestin2 recruitment to μ-OR. In the parental HEK293A cells, fentanyl and loperamide stimulation led to similar maximum responses (E_{max}), whereas DAMGO and morphine induced higher and lower E_{max}, respectively (**Fig. 3**). Based on the complete dependence of μ-OR internalization on β-arrestin (**Fig. 2**), we expected a strong correlation between the μ-OR internalization and β-arrestin2 recruitment. In contrast to this, β-arrestin2 recruitment was unchanged in the ΔGRK2 and/or -3 cell lines, with the exception of the ΔGRK3 cell line where DAMGO stimulation led to a 40% increased recruitment (**Fig. 3, Table 2**). The μ-OR surface expression was the same in all cell lines (**Fig. 3e**) and the ΔGRK cells were still sensitive to GRK2 or -3 overexpression (**Supplementary Fig. S3**). Indeed, rescue expression of either GRK2 or GRK3 led to a significant increase in β-arrestin2 recruitment in the three ΔGRK cell lines for all the ligands. Notably, overexpression of GRK2 and GRK3, promoted morphine-induced β-arrestin2 recruitment to levels similar to loperamide. These data indicate that although GRK2 and GRK3 can promote the recruitment of β-arrestin2 to μ-OR, they are not essential for this recruitment in HEK293 cells. Taken with the results obtained for the internalization, these data also indicate that while it is necessary, the recruitment of β-arrestin2 is not sufficient to promote an efficient internalization.

Bias towards β-arrestin2 recruitment vs. internalization in ΔGRK2/3 cells

To assess whether a bias between μ-OR internalization and β-arrestin2 recruitment was detectable in the genome-edited cells compared to the parental cells, we calculated the differences between the transduction coefficients (**Fig. 4**). These calculations showed a significant bias towards β-arrestin2 recruitment in the ΔGRK2/3 cells compared to the parental cells, when stimulated with DAMGO or loperamide. When calculating the bias for morphine or fentanyl-stimulated cells, no significance was obtained between the cell lines due to higher variation. Yet, a tendency towards β-arrestin2 recruitment bias was observed for fentanyl-stimulated μ-ORs in all the genome-edited cells compared to the parental cells. This analysis is consistent with the larger reductions in internalization than in β-arrestin2 recruitment that we observed upon deleting GRK2 and/or -3.

Similar effects of genetic deletion and pharmacological inhibition of GRK2/3

The small molecule inhibitor CMPD101 has been shown to selectively inhibit GRK2/3 over GRK1 and GRK5 *in vitro*[27]. We compared the internalization and β-arrestin recruitment results obtained in the ΔGRK2/3 cells with that obtained using the kinase inhibitor. At CMPD101 concentrations ≤ 10 μM, we observed no effect on receptor internalization in absence of agonist (basal internalization) (**Fig. 5a**) or basal β-arrestin2 recruitment (**Fig. 5e**) in the parental HEK293A and ΔGRK2/3 cells. With DAMGO stimulation in the parental cells, we found a concentration dependent decrease in μ-OR internalization plateauing at a level similar to the ΔGRK2/3 cells with an IC_{50} of 1.8 μM (pIC_{50} = 5.79 ± 0.12) (**Fig. 5b**) and in β-arrestin2 recruitment with an IC_{50} of 0.73 μM (pIC_{50} = 6.13 ± 0.14) at CMPD101 concentrations ≤ 10 μM (**Fig. 5f**). The reduction in DAMGO-induced β-arrestin2 recruitment with CMPD101 was minor (25%) and similar to the recruitment in ΔGRK2/3 cells (*P* =

174 0.059, paired t-test). Thus, in this concentration range CMPD101 specifically inhibits GRK2/3 and
175 reaches inhibition comparable to the ΔGRK2/3 cell line at 10 μM.

176 At CMPD101 concentrations ≥ 30 μM decreases in basal and DAMGO-stimulated μ-OR
177 internalization were found both in parental and ΔGRK2/3 cells (**Fig. 5a,b**). Basal β-arrestin2
178 recruitment was increased at CMPD101 concentrations ≥ 30 μM in parental and ΔGRK2/3 cells,
179 whereas no further effects were observed on DAMGO-induced recruitment at high CMPD101
180 concentrations (**Fig. 5e,f**). μ-OR surface expression was similar in the parental and ΔGRK2/3 cells in
181 the internalization experiments (**Fig. 5c**) and 25% higher in the ΔGRK2/3 cells in the β-arrestin2
182 recruitment experiments (**Fig. 5g**). Due to the long-lifetime donor fluorophore with several emission
183 peaks and the homogenous format, the internalization assay is sensitive to compounds that absorb
184 light in most of the visual spectrum. However, the donor signal in absence of acceptor was
185 unaffected by CMPD101 even at concentrations ≥ 30 μM (**Fig. 5d**), demonstrating that the observed
186 effects at high concentrations were not due to optical interference with the internalization assay.
187 We conclude that CMPD101 at concentrations above ≥ 30 μM has a non-GRK2/3 regulatory effect
188 on basal μ-OR β-arrestin2 recruitment and internalization and DAMGO-stimulated μ-OR
189 internalization.

190

191 **Discussion**

192 Compelling evidence on the importance of GRKs in μ-OR pharmacology has increased over the
193 years. Yet, most of these studies has relied on methods either overexpressing dominant negative
194 forms of the protein of interest or silencing with siRNAs, possibly leading to undesired effects of
195 overexpression or incomplete removal of the target protein[33]. Genome editing is a promising
196 alternative to these approaches for investigating their role as potential modulators of GPCR

function. In this study we have generated genome-edited HEK293 cells and used them to dissect the role of GRK2 and GRK3 in μ-OR internalization and β-arrestin2 recruitment.

Previous studies have demonstrated that GRK2 and GRK3 affect the phosphorylation state of the ^{375}STANT^{379} motif in mouse μ-OR[19,20,23], and this region has been directly linked to the regulation of μ-OR internalization by mutational studies[20,21]. Here, we demonstrate that our ΔGRK2, ΔGRK3 and ΔGRK2/3 cell lines are excellent novel tools to dissect the role of these GRK subtypes in DAMGO, fentanyl and loperamide-induced μ-OR internalization. Double KO of GRK2/3 had an additive effect on μ-OR internalization with a significant reduction for DAMGO, fentanyl and loperamide-induced μ-OR internalization. No statistically significant difference could be reached for morphine-induced μ-OR internalization, however this agonist induces low μ-OR internalization and thereby the effects could be masked by the small assay window. Our study also shows that there are additional factors controlling μ-OR internalization, since deletion of GRK2/3 did not fully inhibit μ-OR internalization. There is limited evidence suggesting that GRK5 or GRK6 could be responsible for this: μ-OR internalization is sensitive to GRK5 and GRK6 overexpression[13,22] and GRK5 has been shown to be important in HEK293 cells and mouse brain for morphine-induced phosphorylation of Ser375[23], which is a critical residue in initiating further C-terminal μ-OR phosphorylation[20]. In contrast, DAMGO-induced phosphorylation of the C-terminal region of μ-OR was shown to be unaffected by knockdown of GRK5 and GRK6[20,23] and fentanyl-induced Ser375 phosphorylation was unchanged in mice lacking GRK5[12], so the roles of GRK5 and GRK6 might depend on the GRK expression levels in an individual cell. Several other kinases and enzymes have been proposed to regulate μ-OR internalization, including phospholipase D2 (PLD2) and protein kinase C (PKC)[5], but more studies are required to determine their role relative to the GRKs. Our successful generation of the ΔGRK2, ΔGRK3 and ΔGRK2/3 cell lines demonstrate the utility in this approach and calls for generation of

additional cell lines with KO of other kinases to dissect other contributors to μ-OR internalization in the future.

Since agonist-induced μ-OR internalization was shown to be fully dependent on the presence of β-arrestins (**Fig. 2**), we speculated that β-arrestin2 recruitment likewise would be affected by GRK2/3 removal. Surprisingly, β-arrestin2 recruitment was not significantly reduced for any of the agonist stimulations in the ΔGRK2 and/or -3 cells (**Fig. 3, Table 2**). β-arrestin2 recruitment was actually increased slightly but significantly in ΔGRK3 cells when stimulated with DAMGO, which is likely due to competition of GRK3 with GRK2 or another kinase that is more efficient at inducing β-arrestin2 recruitment. Treating the parental cells with the small molecule GRK2/3 inhibitor, CMPD101, showed a similar tendency upon stimulation with DAMGO, namely 60% reduction in internalization and only 25% reduction for β-arrestin2 recruitment (**Fig. 5b,f**). Previous studies have shown, that alanine substitutions of serine and threonine residues in the ^{375}STANT^{379} motif lead to a reduction in the agonist-mediated β-arrestin2 recruitment[21,34], and that residues in this motif are specifically phosphorylated by GRK2 and GRK3[20,23,34]. Since this study was performed on the unmodified μ-OR, it cannot be excluded that there could occur redundant phosphorylation by other kinases, as the μ-OR has been described to be phosphorylated by many different kinases[5], and thereby retain the β-arrestin2 recruitment. While most of the studies mentioned above used the mouse μ-OR, the human μ-OR was used in this study. However, the STANT motif is fully conserved in human μ-OR and the G protein activation and β-arrestin recruitment properties are very similar for mouse and human μ-OR[24,35], so species differences are unlikely to explain the observed differences.

The predominant paradigm of arrestin binding to a GPCR is a two-step model where a pre-complex is formed by binding of arrestin to the phosphorylated GPCR C-tail, followed by major

conformational changes in arrestin leading to a high affinity interaction with the core of the receptor 7TM bundle[36–40]. Different arrestin conformations can result from this encounter depending on the receptor, agonist and the available kinases[41–44] and the arrestin conformation correlates with the trafficking properties of the receptor[44]. Accordingly, we hypothesize, that full phosphorylation of the μ-OR is necessary in order for β-arrestin to be recruited and undergo the full conformational change to mediate receptor internalization, as μ-OR internalization is dramatically reduced in the ΔGRK2/3 cells, however β-arrestin2 might still be able to be recruited to a partially phosphorylated μ-OR but not undergo the full activation necessary to mediate internalization. It should be noted that although our study shows that GRK2 and GRK3 are not necessary for recruitment of β-arrestin2 in HEK293 cells, our rescue experiments here and in a previous study[24] have shown that GRK2 and GRK3 can promote β-arrestin recruitment, so they could be important in other cells.

An alternative arrestin binding and activation model has also been described where arrestin only engages the core of the receptor 7TM bundle[45–48]. Since we measure plasma membrane recruitment and not activation of β-arrestin2 this alternative model provides two additional possible explanations for our observations: (i) Stabilization of an active arrestin conformation is less efficient for the core interaction compared to the core and tail interaction[47] and that could explain why we see similar recruitment of β-arrestin2 but reduced internalization. (ii) Core interactions were shown to result in transient receptor interactions where β-arrestin is retained at the plasma membrane for several receptors, including μ-OR[46,48,49] which results in reduced internalization but smaller changes in plasma membrane localization of β-arrestin compared to core and tail interaction in agreement with our studies.

Although using CRISPR/Cas9 genome editing to generate cell lines lacking specific proteins has several advantages over conventional methods for interrogating protein function, it has also been

criticized for potentially selecting clones that have compensated for the lack of the deleted protein[50]. We addressed this concern by transient expression of the deleted proteins and by pharmacological inhibition with CMPD101. Transient expression of GRK2 or GRK3 showed that μ-OR in the genome-edited cells was still sensitive to regulation by GRK2 and GRK3. Comparison with pharmacological inhibition is an alternative way to characterize genome-edited cells if a specific and potent inhibitor exists. We compared the μ-OR internalization and β-arrestin2 recruitment in the ΔGRK2/3 cells with the effect of the inhibitor CMPD101 on the parental cells and found highly similar results. Collectively, these results demonstrate that there are no significant compensatory mechanisms in the ΔGRK2/3 cells of relevance to the μ-OR functions studied here and confirms the utility of CMPD101 as a GRK2/3 selective pharmacological tool in concentrations up to 10 μM. Our ΔGRK2/3 cells also proved to be a powerful tool to study specificity of GRK inhibitors as we could demonstrate off-target effects of CMPD101 at concentrations ≥ 30 μM, which is a concentration range commonly used to inhibit GRK2/3[28,34], thus cautioning the use of such high concentrations in future studies.

In conclusion, we have generated novel ΔGRK2, ΔGRK3 and ΔGRK2/3 cell lines in the highly utilized HEK293A cell background. These cell lines complement the range of G protein and β-arrestin cell lines generated by Dr. Asuka Inoue[51] and thus expand this highly efficient tool box to study intracellular proteins involved in GPCR function and signaling. Here, we demonstrate the utility of the cell lines to study μ-OR mediated β-arrestin2 recruitment to the cell membrane and μ-OR internalization, but we envision that the cell lines could be used for a range of other studies and thus welcome all requests to obtain the ΔGRK2, ΔGRK3 and ΔGRK2/3 cell lines for future studies.

Methods

Materials

Dulbeccos's modified Eagle medium (DMEM, Cat# 61965-026), fetal bovine serum (FBS), Opti-MEM, Penicillin-Streptomycin, Dulbecco's phosphate buffered saline (DPBS, Cat# 14190-144), Hank's balanced salt solution (HBSS, Cat# 14175-053), restriction endonucleases, TOPO TA cloning kit for sequencing including TOP10 *E. coli.*, FastAP alkaline phosphatase, Pierce BCA Protein Assay Kit, dithiothreitol, PageRuler Plus Prestained Protein Ladder (10 to 250 kDa), Pierce 10x Tris-Glycine SDS Buffer, NuPAGE LDS Sample buffer (4x), SuperSignal West Pico PLUS and ELISA Femto chemiluminescent substrates, and Pluronic F-68 non-ionic surfactant were purchased from Thermo Fisher Scientific (Waltham, MA, USA). QuickExtract DNA Extraction Solution was purchased from Lucigen Corporation (WI, USA) and TEMPase Hot Start DNA Polymerase from Ampliqon (Odense, Denmark). Anti-GRK2 antibody (Cat# MAB43391, RRID:AB_2818985) was from R&D Systems (Minneapolis, MN, USA), anti-GRK3 antibody (Cat# 80362, RRID:AB_2799951) and anti-rabbit IgG antibody conjugated to horseradish peroxidase (HRP) (Cat# 7074, RRID:AB_2099233) were from Cell Signaling Technology (Danvers, MA, USA), anti-GAPDH (Cat# NB600-502, RRID:AB_10077682) antibody was from Novus Biologicals (Centennial, CO, USA) and anti-mouse IgG antibody conjugated to HRP (Cat# P0447, RRID:AB_2617137) was from Agilent Technologies (Santa Clara, CA, USA). Mini-PROTEAN TDX Precast Protein Gels and Trans-Blot Turbo RTA Mini PVDF Transfer Kit were purchased from Bio-Rad Laboratories (Hercules, CA, USA). T4 PNK and T4 ligase were purchased from New England Biolabs (Ipswich, MA, USA). Plasmid-Safe ATP-Dependent DNase was purchased from Epicentre Technologies Corp. (Madison, WI, USA). Primers and sgRNA sequences were purchased from TAG Copenhagen (Copenhagen, Denmark). FuGene6 Transfection Reagent was purchased from Promega (Madison, WI, USA). Polyethylenimine (PEI) was purchased from Polysciences Inc.

311 (Warrington, PA, USA). Coelenterazine 400a was purchased from Cayman Chemical Company (Ann
312 Arbor, MI, USA). Tag-lite SNAP Lumi4-Tb was purchased from Cisbio (Codolet, France). DAMGO was
313 purchased from Abcam (Cambridge, United Kingdom). Anti-FLAG M2 antibody (Cat# F3165,
314 RRID:AB_259529), morphine sulfate, fentanyl citrate, and loperamide hydrochloride, RIPA buffer,
315 Cell Dissociation Solution, protease inhibitor cocktail, Trizma base, skim milk powder, and Tween 20
316 were purchased from Sigma-Aldrich (St. Louis, MO, USA). CMPD101 was purchased from Tocris
317 Bioscience (Bristol, UK).
318
319 **Plasmids**
320 The following plasmids were described previously: pcDNA5/FRT/TO-FLAG-μ-OR[22], pcDNA3.1(+)-β-
321 arrestin1 and pcDNA3.1(+)-β-arrestin2[52], pcDNA3.1/Zeo-β-arrestin2-RlucII[53] and pcDNA3.1(+)-
322 rGFP-CAAX[32]. pSpCas9(BB)-2A-GFP (PX458) was a gift from Feng Zhang (Addgene plasmid # 48138;
323 http://n2t.net/addgene:48138; RRID:Addgene_48138) and was described previously[54]. The
324 pcDNA3.1(+)-GRK2 and pcDNA3.1(+)-GRK3 constructs were kind gifts from Novo Nordisk A/S
325 (Maaloev, Denmark).
326
327 **Cell lines and culturing**
328 The parental HEK293A and Δβ-arrestin1/2 cell lines were kind gifts from Dr. Asuka Inoue[31]. All cell
329 lines were cultured in DMEM supplemented with 10% FBS and 100 U/ml Penicillin-Streptomycin at
330 37 °C and 5% CO_2 in a humidified incubator.
331

Design and cloning of sgRNAs

sgRNA sequences were identified using the WTSI Genome Editing (WGE) tool by screening exonic regions of the genes *ADRBK1* (RefSeq: NC_000011.10) or *ADRBK2* (RefSeq: NC_000022.11) encoding GRK2 and GRK3, respectively. sgRNAs with low predicted off target effects and binding sites upstream of regions encoding catalytic sites in the GRK proteins were chosen, resulting in the sgRNA sequence 5'-CTTCGACTCATACATCATGA-3' binding in exon 4 within the *ADRBK1* gene and the sgRNA sequence 5'-ATTATTGGACGAGGAGGATT-3' binding in exon 8 within the *ADRBK2* gene. Overhangs for cloning into a BsbI restriction site were placed in the ends of the sgRNAs. sgRNAs were prepared for cloning by incubating 100 μM of reverse complementary strands with T4 PNK in a thermocycler at 37 °C for 30 minutes followed by a 5-minute incubation at 95 °C and ramping down to 25 °C with 5 °C/min. The double stranded sgRNAs were ligated into BsbI digested pSpCas9(BB)-2A-GFP by incubating with T4 DNA ligase for 1 hour at 22 °C. To remove excess non-ligated DNA, the samples were treated with Plasmid-Safe ATP-Dependent DNase for 30 minutes at 37 °C.

Generation and validation of CRISPR-Cas9 KO cell lines

HEK293A cells were seeded at a density of 2×10^5 cells/well in a 6-well plate and incubated at 37 °C and 5% CO_2 in a humidified incubator. Twenty-four hours later cells were transfected with 500 ng/well pSpCas9(BB)-2A-GFP encoding the sgRNAs using FuGene6 as the transfection reagent and the cells were incubated at 37 °C and 5% CO_2 in a humidified incubator. Forty-eight hours later, the cells were harvested by trypsination and sorted based on their GFP expression with fluorescence assisted cell sorting (FACS) using a MoFlo Astrios Cell Sorter (Beckman Coulter, Brea, CA, USA). Cells were seeded in 96-well culture plates to isolate single clones and were incubated at 37 °C and 5% CO_2 in a humidified incubator until ~70% confluent.

355

356 **IDAA**

357 Single clones were harvested from 96-well plates by trypsination and DNA was extracted using
358 QuickExtract followed by cell lysis (20 min at 65 °C, 10 min at 98 °C) as described previously[55]. A tri-
359 primer PCR described previously[56] was performed using TEMPase Hot Start DNA Polymerase. To
360 amplify the *ADRBK1* locus, the following primers and concentrations were used: 0.05 µM forward
361 primer (5'-AGCTGACCGGCAGCAAAATTGCCAGGCCCTTGGTGGAATTCTATG-3'), 0.5 µM reverse
362 primer (5'-GGACATGCTCAGTGGCACTCTTC-3') and 0.5 µM FAM forward primer (5'-6-FAM-
363 AGCTGACCGGCAGCAAAATTG-3'). For amplification of the *ADRBK2* locus following primers and
364 concentrations were used: 0.05 µM forward primer (5'-
365 AGCTGACCGGCAGCAAAATTGCCTGGGGCATCTCATCCTTCAGC-3'), 0.5 µM reverse primer (5'-
366 CGCCCGGCCTACAGCTTATTTC-3') and 0.5 µM FAM forward primer (5'-6-FAM-
367 AGCTGACCGGCAGCAAAATTG-3'). A touchdown thermocycling program was used with denaturation
368 at 95 °C for 15 min followed by 15 cycles with an annealing temperature of 72 °C ramping down to
369 58 °C with 1 °C/cycle. Subsequent 24 cycles with 58 °C as annealing temperature was performed
370 ending with elongation at 72 °C for 20 min. For both annealing cycles, denaturation and elongation
371 was performed at 95 °C and 72 °C for 30 s, respectively. IDAA on the resulting PCR products was
372 executed by COBO Technologies Aps (Copenhagen, Denmark).

373

374 **Genome sequencing**

375 DNA from the genome-edited cell lines was extracted as described above for IDAA. The *ADRBK1* or
376 *ADRBK2* regions targeted by the sgRNA were PCR amplified with the forward primers 5'-
377 CCAGGCCCTTGGTGGAATTCTATG-3' (*ADRBK1*) and 5'-CCTGGGGCATCTCATCCTTCAGC-3' (*ADRBK2*)

and the same reverse primers as used for IDAA. PCR products were cloned into the pCR4-TOPO TA vectors using the TOPO TA cloning kit and used to transform TOP10 bacteria. DNA from 5-10 single clones was sequenced for each genome-edited cell line to determine the modifications for all alleles.

Western blot

Genome-edited HEK293A cells were incubated in 15-cm culture dishes at 37 °C and 5% CO_2 in a humidified incubator until ~90% confluency and harvested with ice cold Cell Dissociation Solution. Cells were centrifuged in a tabletop centrifuge at 4 °C for 5 min at 500 x *g*. Whole cell lysates were prepared from pellets by resuspending in RIPA buffer containing protease inhibitor cocktail. Cells were pulse sonicated for 30 s and incubated with end-over-end rotation at 4 °C for 60 min. Lysates were centrifuged in a tabletop centrifuge at 4 °C for 10 min at 15,000 x *g*. The supernatant was transferred to a clean microcentrifuge tube and the protein concentrations were determined using Pierce BCA Protein Assay Kit according to the manufacturer's instructions. The absorbance of the samples was measured at 562 nm on an EnSpire Multimode Plate Reader (PerkinElmer), and the values were converted to protein concentrations by interpolation from a bovine serum albumin (BSA) standard curve. Western blot samples were prepared with 50 µg protein in NuPAGE LDS Sample Buffer supplemented with 100 µM dithiothreitol (DTT) and heated for 30 s at 50 °C. Subsequently they were incubated for 15 minutes at room temperature and electrophoresed for 40 min at 200 V. Proteins were transferred onto a polyvinylidene difluoride (PVDF) membrane followed by one hour blocking with 5% skim milk in Tris buffered saline with Tween 20 (TBS-T; 10 mM Tris pH 7.4, 150 mM NaCl, 0.1% Tween 20). The PVDF membrane was incubated over night with anti-GRK2 (0.1 µg/ml in TBS-T with 5% skim milk), anti-GRK3 (1:2000 in TBS-T with 5% skim milk) or anti-GAPDH (1:5000 in TBS-T with 1% BSA) at 4 °C. The membranes were washed three times with TBS-T and

401 incubated with secondary antibodies for one hour at room temperature with gentle agitation
402 followed by three washes with TBS-T. Blots were developed with HRP substrate and imaged with a
403 FluorChem HD2 system (ProteinSimple, San Jose, CA, USA).
404
405 **β-arrestin2 recruitment**
406 Parental HEK293A cells or genome-edited cells were transfected with PEI for β-arrestin2
407 recruitment experiments as previously described[32] with 20 ng/ml β-arrestin2-RlucII (BRET donor),
408 500 ng/ml rGFP-CAAX (BRET acceptor), pcDNA5/FRT/TO-FLAG-μ-OR and pcDNA3.1(+) for 500,000
409 cells/ml. The amount of pcDNA5/FRT/TO-FLAG-μ-OR was adjusted for each cell line to equalize the
410 expression: 15 ng/ml for parental HEK293A and ΔGRK2, 20 ng/ml for ΔGRK2/3 and 30 ng/ml for
411 ΔGRK3. The total DNA amount was adjusted to 1 μg/ml with pcDNA3.1(+). 32,000 cells mixed with
412 DNA and PEI were added to each well in poly-D-lysine-coated white, opaque CulturPlate-96 96-well
413 plates (PerkinElmer, Waltham, MA, USA). Forty-eight hours after transfection, cells were washed
414 and incubated in assay buffer (HBSS supplemented with 1 mM $CaCl_2$, 1 mM $MgCl_2$, 20 mM HEPES
415 and 0.01% Pluronic F-68, pH 7.4) for 30 min before addition of agonists. For experiments with
416 CMPD101, cells were incubated for an additional 30 min in presence of CMPD101 before agonist
417 addition. After 1 h agonist incubation at 37 °C, coelenterazine 400a was added to a final
418 concentration of 2.5 μM and 2 min later BRET was measured on an EnVision 2104 Multilabel Reader
419 (PerkinElmer) equipped with $BRET^2$ filters: 410/80 nm (donor) and 515/30 nm (acceptor). $BRET^2$
420 ratios were calculated as the ratio of acceptor and donor emission (515 nm/410 nm). For
421 concentration-response curves the buffer response was subtracted.
422

ELISA

Receptor surface expression in β-arrestin2 recruitment experiments was determined using enzyme-linked immunosorbent assay (ELISA) as previously described[57] with anti-FLAG as primary antibody in a 1:1000 dilution.

TR-FRET real-time internalization

Parental HEK293A cells or genome-edited cells were transfected with PEI for real-time internalization experiments with different amounts of pcDNA5/FRT/TO-FLAG-μ-OR depending on the cell line (same amounts for each cell line as in β-arrestin2 recruitment experiments) to equalize expression and the total DNA amount was adjusted to 1 μg/ml with pcDNA3.1(+). 14,000 cells mixed with DNA and PEI were added to each well in a poly-D-lysine-coated white, opaque 384-well plates (Greiner Bio-One, Kremsmünster, Austria). Forty-eight hours after transfection, cells were labeled with 10 μl Tag-lite Lumi4-Tb for 60 min at 37 °C in Opti-MEM. After labeling, cells were washed twice with assay buffer (HBSS supplemented with 1 mM $CaCl_2$, 1 mM $MgCl_2$, 20 mM HEPES and 0.01% Pluronic F-68, pH 7.4) and incubated for 5 min with 10 μl of 100 μM fluorescein-O'-acetic acid. The donor signal was measured before removing the second wash from the plate and used as a measure of the μ-OR surface expression. For experiments with CMPD101, the compound was added together with fluorescein-O'-acetic acid and the incubation was extended to 30 min. 10 μl agonist was then added and internalization was read immediately after for 90 min in 6 min intervals on an EnVision 2104 Multilabel Reader using a 340/60 nm excitation filter and emission was recorded through 520/8 nm (acceptor) and 615/8.5 nm (donor) emission filters. Internalization ratios were calculated as the ratio of donor over acceptor emission (615 nm/520 nm) for real-time internalization curves. For concentration-response curves the area under the real-time internalization curves was

446 calculated and the buffer response subtracted. The IC_{50} of CMPD101 inhibition of internalization
447 was determined by fitting the concentration-response curve obtained by subtracting the DAMGO −
448 buffer response in ΔGRK2/3 cells from the DAMGO − buffer response in parental cells.
449
450 **Data analysis and statistics**
451 Data are presented as mean ± SEM of n ≥ 3 independent experiments. Results were analyzed using
452 Prism 7.0 (GraphPad Software, San Diego, CA, USA). Differences were determined with regular or
453 repeated measures one-way ANOVA with Dunnett's multiple comparisons test or paired t-test on
454 non-normalized data; $P < 0.05$ was considered significant. In Fig. 1b where data was compared to a
455 reference value without variance (100 ± 0), observations were compared to the reference value
456 using a one sample t-test and the cutoff for what was considered a significant difference was
457 adjusted to $P < 0.05/n$ (n represents the number of compared observations) to account for multiple
458 comparisons. Transduction coefficients used for quantification of ligand bias were determined by
459 fitting to the operational model of agonism as previously published[22].
460
461 **Data Availability**
462 The datasets generated during the current study are available from the corresponding authors on
463 reasonable request.
464
465
466 **References:**
467 1. Hauser, A. S., Attwood, M. M., Rask-Andersen, M., Schiöth, H. B. & Gloriam, D. E. Trends in
468 GPCR drug discovery: new agents, targets and indications. *Nat. Rev. Drug Discov.* **16**, 829–

842 (2017).

2. Hanyaloglu, A. C. & von Zastrow, M.. Regulation of GPCRs by endocytic membrane trafficking and its potential implications. *Annu. Rev. Pharmacol. Toxicol.* **48**, 537–568 (2008).

3. Dahan, A. *et al.* Anesthetic potency and influence of morphine and sevoflurane on respiration in mu-opioid receptor knockout mice. *Anesthesiology* **94**, 824–832 (2001).

4. Charbogne, P., Kieffer, B. L. & Befort, K. 15 years of genetic approaches in vivo for addiction research: Opioid receptor and peptide gene knockout in mouse models of drug abuse. *Neuropharmacology* **76**, 204–217 (2014).

5. Williams, J. T. *et al.* Regulation of μ-opioid receptors: Desensitization, phosphorylation, internalization, and tolerance. *Pharmacol. Rev.* **65**, 223–254 (2013).

6. Wang, Z., Arden, J. & Sadee, W. Basal phosphorylation of μ opioid receptor is agonist modulated and Ca^{2+}-dependent. *FEBS Lett.* **387**, 53–57 (1996).

7. Zhang, L. *et al.* Differential μ opiate receptor phosphorylation and desensitization induced by agonists and phorbol esters. *J. Biol. Chem.* **271**, 11449–11454 (1996).

8. Yu, Y. *et al.* μ opioid receptor phosphorylation, desensitization, and ligand efficacy. *J. Biol. Chem.* **272**, 28869–28874 (1997).

9. Deng, H. B. *et al.* Role for the C-terminus in agonist-induced μ opioid receptor phosphorylation and desensitization. *Biochemistry* **39**, 5492–5499 (2000).

10. Raehal, K. M., Schmid, C. L., Groer, C. E. & Bohn, L. M. Functional selectivity at the μ-opioid receptor: implications for understanding opioid analgesia and tolerance. *Pharmacol. Rev.* **63**, 1001–1019 (2011).

11. Terman, G. W. *et al.* G-protein receptor kinase 3 (GRK3) influences opioid analgesic tolerance but not opioid withdrawal. *Br. J. Pharmacol.* **141**, 55–64 (2004).

12. Glück, L. *et al.* Loss of morphine reward and dependence in mice lacking G protein-coupled receptor kinase 5. *Biol. Psychiatry* **76**, 767–774 (2014).

13. Raehal, K. M. *et al.* Morphine-induced physiological and behavioral responses in mice lacking G protein-coupled receptor kinase 6. *Drug Alcohol Depend.* **104**, 187–196 (2009).

14. Jaber, M. *et al.* Essential role of beta-adrenergic receptor kinase 1 in cardiac development and function. *Proc. Natl. Acad. Sci.* **93**, 12974–12949 (1996).

15. Li, A. H. & Wang, H.-L. G protein-coupled receptor kinase 2 mediates μ-opioid receptor desensitization in GABAergic neurons of the nucleus raphe magnus. *J. Neurochem.* **77**, 435–444 (2001).

16. Bailey, C. *et al.* Involvement of PKCα and G-protein-coupled receptor kinase 2 in agonist-selective desensitization of μ-opioid receptors in mature brain neurons. *Br. J. Pharmacol.* **158**, 157–164 (2009).

17. Zhang, J. *et al.* Role for G protein-coupled receptor kinase in agonist-specific regulation of mu-opioid receptor responsiveness. *Proc. Natl. Acad. Sci.* **95**, 7157–7162 (1998).

18. McPherson, J. *et al.* μ-opioid receptors: correlation of agonist efficacy for signalling with ability to activate internalization. *Mol. Pharmacol.* **78**, 756–766 (2010).

19. Schulz, S. *et al.* Morphine induces terminal μ-opioid receptor desensitization by sustained phosphorylation of serine-375. *EMBO J.* **23**, 3282–3289 (2004).

20. Just, S. *et al.* Differentiation of opioid drug effects by hierarchical multi-site phosphorylation. *Mol. Pharmacol.* **83**, 633–639 (2013).

21. Lau, E. K. *et al.* Quantitative encoding of the effect of a partial agonist on individual opioid receptors by multisite phosphorylation and threshold detection. *Sci. Signal.* **4**, ra52–ra52 (2011).

22. Pedersen, M. F. *et al.* Biased agonism of clinically approved μ-opioid receptor agonists and TRV130 is not controlled by binding and signaling kinetics. *Neuropharmacology*, doi:10.1016/J.NEUROPHARM.2019.107718

23. Doll, C. *et al.* Deciphering μ-opioid receptor phosphorylation and dephosphorylation in HEK293 cells. *Br. J. Pharmacol.* **167**, 1259–1270 (2012).

24. Ehrlich, A. T. *et al.* Biased signaling of the mu opioid receptor revealed in native neurons. *iScience* **14**, 47–57 (2019).

25. Celver, J., Xu, M., Jin, W., Lowe, J. & Chavkin, C. Distinct domains of the μ-opioid receptor control uncoupling and internalization. *Mol. Pharmacol.* **65**, 528–537 (2004).

26. Ikeda, S., Manami, K. & Fujiwara, S., inventors; Takeda Pharmaceutical Company Ltd. Ikeda S., Keneko M., and Fujiwara S., assignees. Cardiotonic agent comprising GRK inhibitor. World patent WO2007034846. (2007).

27. Thal, D. M., Yeow, R. Y., Schoenau, C., Huber, J. & Tesmer, J. J. G. Molecular mechanism of selectivity among G protein-coupled receptor kinase 2 inhibitors. *Mol. Pharmacol.* **80**, 294–303 (2011).

28. Lowe, J. D. *et al.* Role of G protein-coupled receptor kinases 2 and 3 in μ-opioid receptor desensitization and internalization. *Mol. Pharmacol.* **88**, 347–356 (2015).

29. Roed, S. N. *et al.* Real-time trafficking and signaling of the glucagon-like peptide-1 receptor. *Mol. Cell. Endocrinol.* **382**, 938–949 (2014).

30. Levoye, A. *et al.* A Broad G Protein-Coupled Receptor Internalization Assay that Combines SNAP-Tag Labeling, Diffusion-Enhanced Resonance Energy Transfer, and a Highly Emissive Terbium Cryptate. *Front. Endocrinol. (Lausanne).* **6**, 167 (2015).

31. O'Hayre, M. *et al.* Genetic evidence that β-arrestins are dispensable for the initiation of β2-

538 adrenergic receptor signaling to ERK. *Sci. Signal.* **10**, eaal3395 (2017).

539 32. Namkung, Y. *et al.* Monitoring G protein-coupled receptor and β-arrestin trafficking in live
540 cells using enhanced bystander BRET. *Nat. Commun.* **7**, 1–12 (2016).

541 33. Boutros, M. & Ahringer, J. The art and design of genetic screens: RNA interference. *Nat.*
542 *Rev. Genet.* **9**, 554–566 (2008).

543 34. Miess, E. *et al.* Multisite phosphorylation is required for sustained interaction with GRKs
544 and arrestins during rapid μ-opioid receptor desensitization. *Sci. Signal.* **11**, eaas9609
545 (2018).

546 35. Benredjem, B. *et al.* Exploring use of unsupervised clustering to associate signaling profiles
547 of GPCR ligands to clinical response. *Nat. Commun.* **10**, (2019).

548 36. Schröder, K., Pulvermüller, A. & Hofmann, K. P. Arrestin and its splice variant Arr 1–370A (p
549 44). Mechanism and biological role of their interaction with rhodopsin. *J. Biol. Chem.* **277**,
550 43987–43996 (2002).

551 37. Kumari, P. *et al.* Functional competence of a partially engaged GPCR–β-arrestin complex.
552 *Nat. Commun.* **7**, 13416 (2016).

553 38. Sommer, M. E., Farrens, D. L., McDowell, J. H., Weber, L. A. & Smith, W. C. Dynamics of
554 arrestin-rhodopsin interactions. *J. Biol. Chem.* **282**, 25560–25568 (2007).

555 39. Kim, M. *et al.* Conformation of receptor-bound visual arrestin. *Proc. Natl. Acad. Sci.* **109**,
556 18407–18412 (2012).

557 40. Szczepek, M. *et al.* Crystal structure of a common GPCR-binding interface for G protein and
558 arrestin. *Nat. Commun.* **5**, 4801 (2014).

559 41. Shukla, A. K. *et al.* Distinct conformational changes in β-arrestin report biased agonism at
560 seven-transmembrane receptors. *Proc. Natl. Acad. Sci.* **105**, 9988–9993 (2008).

42. Zimmerman, B. *et al.* Differential β-arrestin-dependent conformational signaling and cellular responses revealed by angiotensin analogs. *Sci. Signal.* **5**, (2012).

43. Nuber, S. *et al.* β-Arrestin biosensors reveal a rapid, receptor-dependent activation/deactivation cycle. *Nature* **531**, 661–664 (2016).

44. Lee, M. H. *et al.* The conformational signature of β-arrestin2 predicts its trafficking and signalling functions. *Nature* **531**, 665–668 (2016).

45. Jala, V. R., Shao, W.-H. & Haribabu, B. Phosphorylation-independent β-arrestin translocation and internalization of leukotriene B4 receptors. *J. Biol. Chem.* **280**, 4880–4887 (2005).

46. Jung, S.-R., Kushmerick, C., Seo, J. B., Koh, D.-S. & Hille, B. Muscarinic receptor regulates extracellular signal regulated kinase by two modes of arrestin binding. *Proc. Natl. Acad. Sci.* **114**, E5579–E5588 (2017).

47. Latorraca, N. R. *et al.* Molecular mechanism of GPCR-mediated arrestin activation. *Nature* **557**, 452–456 (2018).

48. Eichel, K. *et al.* Catalytic activation of β-arrestin by GPCRs. *Nature* **557**, 381–386 (2018).

49. Eichel, K., Jullié, D. & von Zastrow, M. β-Arrestin drives MAP kinase signalling from clathrin-coated structures after GPCR dissociation. *Nat. Cell Biol.* **18**, 303–310 (2016).

50. Luttrell, L. M. *et al.* Manifold roles of β-arrestins in GPCR signaling elucidated with siRNA and CRISPR/Cas9. *Sci. Signal.* **11**, eaat7650 (2018).

51. Milligan, G. & Inoue, A. Genome editing provides new insights into receptor-controlled signalling pathways. *Trends Pharmacol. Sci.* **39**, 481–493 (2018).

52. Gabe, M. B. N. *et al.* Human GIP(3-30)NH 2 inhibits G protein-dependent as well as G protein-independent signaling and is selective for the GIP receptor with high-affinity binding to primate but not rodent GIP receptors. *Biochem. Pharmacol.* **150**, 97–107 (2018).

584 53. Quoyer, J. *et al.* Pepducin targeting the C-X-C chemokine receptor type 4 acts as a biased
585 agonist favoring activation of the inhibitory G protein. *Proc. Natl. Acad. Sci.* **110**, E5088–
586 E5097 (2013).
587 54. Ran, F. A. *et al.* Genome engineering using the CRISPR-Cas9 system. *Nat. Protoc.* **8**, 2281–
588 2308 (2013).
589 55. Lonowski, L. A. *et al.* Genome editing using FACS enrichment of nuclease-expressing cells
590 and indel detection by amplicon analysis. *Nat. Protoc.* **12**, 581–603 (2017).
591 56. Yang, Z. *et al.* Fast and sensitive detection of indels induced by precise gene targeting.
592 *Nucleic Acids Res.* **43**, e59–e59 (2015).
593 57. Nørskov-Lauritsen, L., Jørgensen, S. & Bräuner-Osborne, H. N-glycosylation and disulfide
594 bonding affects GPRC6A receptor expression, function, and dimerization. *FEBS Lett.* **589**,
595 588–597 (2015).

596

597 **Author contributions:**

598 M.F.P., T.C.M., J.M.M., M.B. and H.B.-O. participated in research design. M.F.P., T.C.M. and S.D.S.
599 conducted experiments. M.F.P., T.C.M. and S.D.S. performed data analysis. M.F.P., T.C.M., S.D.S.
600 and H.B.-O. wrote or contributed to drafting the manuscript. All authors edited and approved the
601 final manuscript.

602

603 **Acknowledgements:**

604 We thank Dr. Asuka Inoue for the HEK293 parental and Δβ-arrestin1/2 cell lines and for fruitful
605 discussions and Jens Peter Stenvang for technical assistance with cell sorting. We also thank Eric
606 Paul Bennett for input related to indel detection by amplicon analysis. H.B.-O. acknowledges

607 financial support from the Independent Research Fund Denmark | Medical Sciences (4183-00131A),
608 the Lundbeck Foundation, the Novo Nordisk Foundation (NNF17OC0027004), the Carlsberg
609 Foundation (CF17-0132) and the Toyota Foundation (9310-F). M.F.P. thank the Oticon Foundation
610 (16-0668) and the Knud Højgaards Foundation (16-02-0142) for financial support. T.C.M.
611 acknowledges funding from the European Union's Horizon2020 research and innovation
612 programme under the Marie Sklodowska-Curie grant agreement No 797497. M.B. acknowledge the
613 financial support from a Canadian Institute for Health Research (CIHR) Foundation grant (FDN-
614 148431). M.B. also holds a Canada Research Chair in Signal Transduction and Molecular
615 Pharmacology.

616

617 **Additional Information**

618 **Supplementary information** accompanies this paper at …

619 **Competing Interests**: The authors declare no competing interests.

620

621 **Figure legends**

622 **Figure 1.** Validation of CRISPR/Cas9 knock-out cell lines. (**a**) Western blot analysis of full-length GRK2
623 or GRK3 expression in parental or genome-edited cell lines with deletion of GRK2, GRK3 or GRK2/3.
624 The anti-GRK2 and anti-GRK3 antibodies target a site C-terminal to the site that is genetically
625 modified. GAPDH expression is detected to ensure equal loading. In cases where samples were not
626 located directly next to each other on the blot, a vertical line on the blot indicates the splice junction.
627 In all comparisons to the reference WT, samples from the genome-edited cells were located on the
628 same blot and treated equally to the reference WT. (**b**) Quantification of anti-GRK2 and anti-GRK3
629 western blots after normalization to the GAPDH signal. Mean ± SEM of 3-7 independent

experiments. Expression in each of the KO cell lines was compared to the parental cells by one sample t-test using a reference value of 100 and the cutoff for what was considered a significant difference was adjusted to $P < 0.05/n$ (n corresponds to the number of observations) to correct for multiple comparisons. ***$P < 0.001/n$.

Figure 2. Agonist-induced internalization of μ-OR in genetically modified cell lines. Internalization of μ-OR in response to a range of concentrations of (**a**) DAMGO, (**b**), fentanyl (**c**) loperamide, or (**d**) morphine in parental HEK293A (WT) cells or HEK293A cell lines with deletion of GRK2 (ΔGRK2), GRK3 (ΔGRK3), GRK2 and -3 (ΔGRK2/3) or β-arrestin1 and -2 (Δβ-Arr1/2). Data represents the mean ± SEM of the area under the curve of 90 min real-time internalization experiments after buffer subtraction from 3-5 independent experiments carried out in duplicate. (**e**) μ-OR cell surface expression determined by measuring donor signals in absence of acceptor. Data represents the mean of individual experiments (circles) as well as the mean ± SEM (columns) from 6-9 independent experiments with 32 replicates per experiment. Expression in each of the knock-out cell lines was compared to the parental cells by one-way ANOVA with Dunnett's multiple comparisons test. **P = 0.001-0.01.

Figure 3. β-arrestin2 recruitment of μ-OR in genetically modified cell lines. Recruitment of β-arrestin2-RlucII to the cell membrane monitored by ebBRET in response to a range of concentrations of (**a**) DAMGO, (**b**) fentanyl, (**c**) loperamide, or (**d**) morphine in parental HEK293A (WT) cells or HEK293A cell lines with deletion of GRK2 (ΔGRK2), GRK3 (ΔGRK3), or GRK2 and -3 (ΔGRK2/3). Data represents the mean ± SEM after buffer subtraction from 3-4 independent experiments carried out in duplicate. (**e**) μ-OR surface expression measured by ELISA and normalized to expression in

parental cells. Data points represent the mean of individual experiments and bars represent the mean ± SEM from six independent experiments performed in triplicate. Expression in each of the knock-out cell lines was compared to the parental cells by one-way repeated measures ANOVA with Dunnett's multiple comparisons test before normalization and no significant differences were found ($P > 0.05$).

Figure 4. Bias profile of μ-OR signaling in GRK2 and/or -3 knock out cells and WT cells. Concentration response curves from μ-OR internalization and β-arrestin2 recruitment experiments were fitted to the operational model of agonism. The $\Delta\log(\tau/K_A)$ was calculated with WT as the reference and the $\Delta\Delta\log(\tau/K_A)$ values by subtracting values obtained for internalization from those obtained in β-arrestin2 recruitment experiments. Bias values are presented from cells stimulated with DAMGO, loperamide, fentanyl and morphine. Data represent the mean ± SEM of 3-4 individual experiments. Statistical significance compared to parental cells was assessed using one-way ANOVA analysis followed by Dunnett's multiple comparisons test.

Figure 5. GRK2/3 inhibition and off-target effects by CMPD101. Effect of a range of CMPD101 concentrations on (**a**) basal (vehicle treated) or (**b**) 100 μM DAMGO induced μ-OR internalization and (**e**) basal (vehicle treated) or (**f**) 150 μM DAMGO stimulated β-arrestin2 recruitment in parental HEK293A (WT) cells or HEK293A cell lines with deletion of GRK2 and -3 (ΔGRK2/3). Data represents the mean ± SEM after buffer (vehicle treated) or vehicle (DAMGO treated) subtraction from 3 independent experiments carried out in duplicate. μ-OR surface expression was determined from donor signals in absence of acceptor for internalization experiments (**c**) and by ELISA for β-arrestin2 recruitment experiments (**g**). Data points represent the mean of individual experiments and bars

676 represent the mean ± SEM from three independent experiments with 32 (internalization) or 3
677 (ELISA) replicates per experiment. In (**g**) data was normalized to expression in parental cells. (**d**)
678 Effect of a range of CMPD101 concentrations on donor signals in absence of acceptor. An unaffected
679 donor signal indicates that the compound does not interfere with the assay. Data represents the
680 mean ± SEM from 3 independent experiments carried out in duplicate. Effect of different CMPD101
681 concentrations on ΔGRK2/3 cells in (**a**), (**b**), (**d**), (**e**) and (**f**) was compared to buffer by one-way
682 repeated measures ANOVA with Dunnett's multiple comparisons test before normalization.
683 Expression in parental and ΔGRK2/3 cells in (**c**) and (**g**) was compared by ratio paired t-test before
684 normalization. **P* = 0.01-0.05, ****P* < 0.001.
685

Table 1. E_{max} (% of parental HEK293A (WT) cells) and pEC_{50} values for μ-OR internalization obtained from fitting concentration-response curves to a four-parameter model of agonism. No fit could be obtained for experiments in cells where β-arrestin1 and -2 had been deleted. E_{max} and pEC_{50} values are the mean of 3-5 independent experiments. E_{max} and pEC_{50} in knock out cells are compared to the parental cells by one-way repeated measures ANOVA with Dunnett's multiple comparisons test before normalization.

	WT				ΔGRK2				ΔGRK3				ΔGRK2/3			
	E_{max}	SEM	pEC_{50}	SEM	E_{max}	SEM	pEC_{50}	SEM	E_{max}	SEM	pEC_{50}	SEM	E_{max}	SEM	pEC_{50}	SEM
DAMGO	100	5	6.44	0.03	52[c]	5	6.27	0.06	77[a]	6	6.43	0.04	31[c]	9	6.14[b]	0.15
Fentanyl	100	5	6.94	0.01	38[c]	5	6.75[c]	0.04	78[a]	5	6.81[c]	0.02	18[c]	6	7.03[a]	0.01
Loperamide	100	8	6.96	0.04	47[c]	7	6.74	0.10	78	8	6.95	0.07	18[c]	17	6.91	0.08
Morphine	100	15	5.65	0.12	84	37	4.65	0.89	71	14	5.84	0.05	38	12	6.02	0.13

[a] P = 0.01-0.05 compared to WT

[b] P = 0.001-0.01 compared to WT

[c] P < 0.001 compared to WT

Table 2. E_{max} (% of parental HEK293A (WT) cells) and pEC_{50} values for μ-OR β-arrestin2 recruitment obtained from fitting concentration-response curves to a four-parameter model of agonism. E_{max} and pEC_{50} values are the mean of 3-4 independent experiments. E_{max} and pEC_{50} in knock out cells are compared to the parental cells by one-way repeated measures ANOVA with Dunnett's multiple comparisons test before normalization.

	WT				ΔGRK2				ΔGRK3				ΔGRK2/3			
	E_{max}	SEM	pEC_{50}	SEM	E_{max}	SEM	pEC_{50}	SEM	E_{max}	SEM	pEC_{50}	SEM	E_{max}	SEM	pEC_{50}	SEM
DAMGO	100	6	6.28	0.06	92	5	6.30	0.02	140[a]	6	6.29	0.02	84	13	6.30	0.06
Fentanyl	100	8	6.72	0.13	97	20	6.52	0.19	108	9	6.84	0.09	78	9	6.83	0.08
Loperamide	100	6	7.11	0.02	84	8	7.07	0.09	117	5	7.11	0.04	94	11	6.99	0.11
Morphine	100	23	5.70	0.29	89	25	5.68	0.65	123	27	5.93	0.49	88	29	5.94	0.24

[a] P = 0.001-0.01 compared to WT

Figure 1

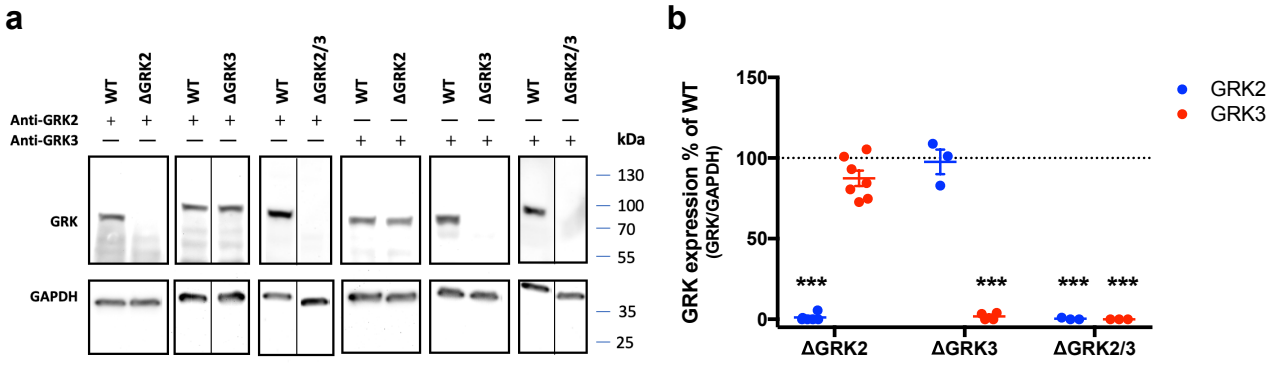

Figure 2

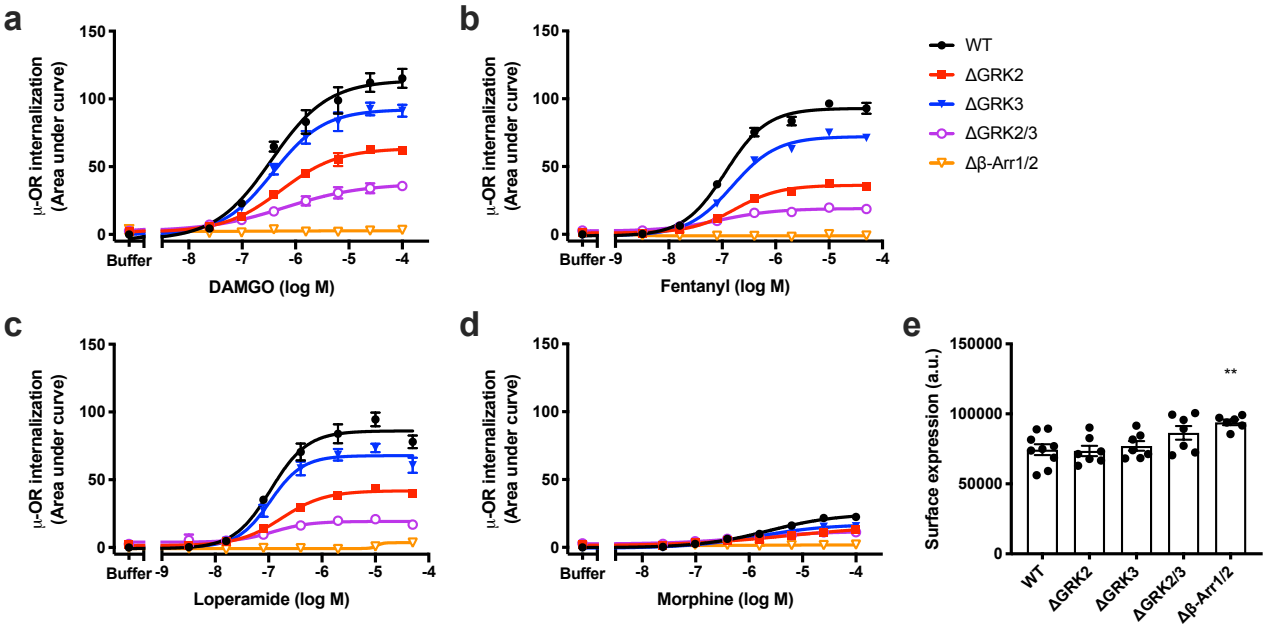

Figure 3

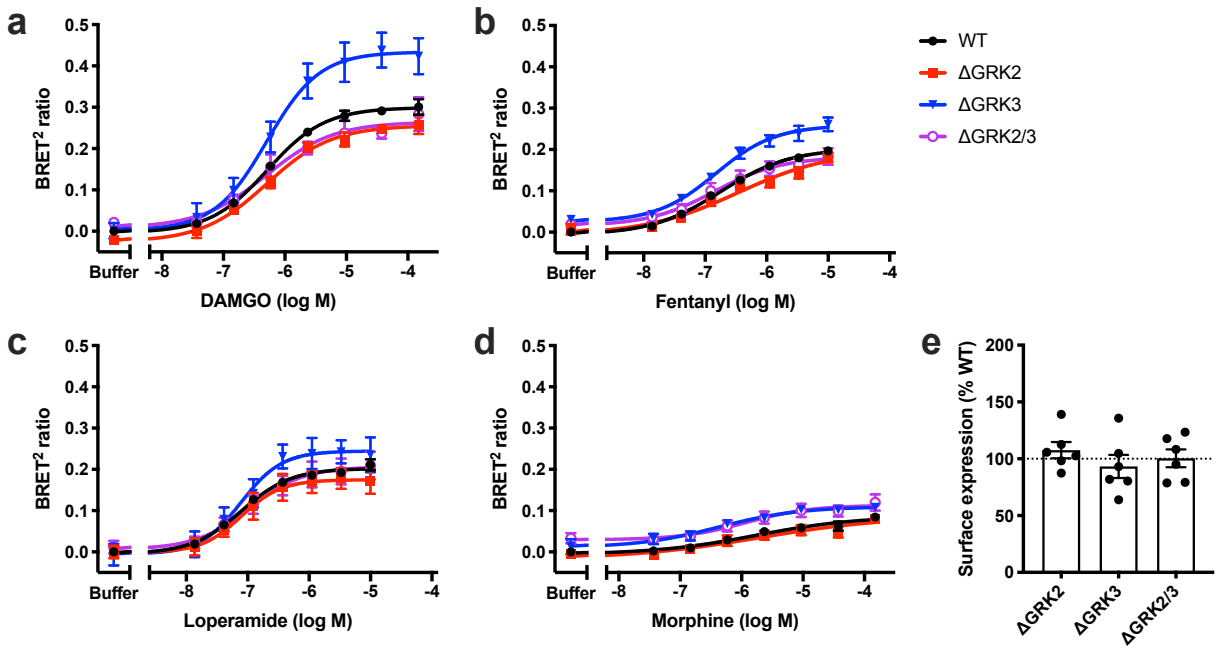

Figure 4

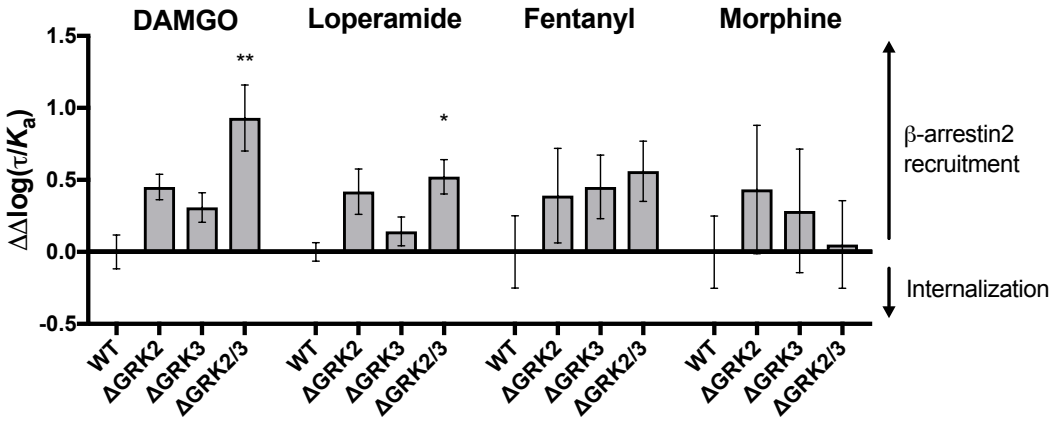

Figure 5